Neurosci Bull February 1, 2013, 29(1): 28–36. http://www.neurosci.cn
DOI: 10.1007/s12264-013-1304-4

·Original Article·

Spatiotemporal dynamics of high-K^+-induced epileptiform discharges in hippocampal slice and the effects of valproate

Jian-Sheng Liu[1], Jing-Bo Li[1], Xin-Wei Gong[2], Hai-Qing Gong[2], Pu-Ming Zhang[2], Pei-Ji Liang[2], Qin-Chi Lu[1]
[1]*Department of Neurology, Renji Hospital, School of Medicine, Shanghai Jiao Tong University, Shanghai 200127, China*
[2]*Department of Biomedical Engineering, Shanghai Jiao Tong University, Shanghai 200240, China*
Corresponding authors: Pei-Ji Liang, Qin-Chi Lu. E-mail: pjliang@sjtu.edu.cn, qinchilu2011@yahoo.com.cn

ABSTRACT

The epileptic seizure is a dynamic process involving a rapid transition from normal activity to a state of hypersynchronous neuronal discharges. Here we investigated the network properties of epileptiform discharges in hippocampal slices in the presence of high K^+ concentration (8.5 mmol/L) in the bath, and the effects of the anti-epileptic drug valproate (VPA) on epileptiform discharges, using a microelectrode array. We demonstrated that epileptiform discharges were predominantly initiated from the stratum pyramidale layer of CA3a–b and propagated bi-directionally to CA1 and CA3c. Disconnection of CA3 from CA1 abolished the discharges in CA1 without disrupting the initiation of discharges in CA3. Further pharmacological experiments showed that VPA at a clinically relevant concentration (100 μmol/L) suppressed the propagation speed but not the rate or duration of high-K^+-induced discharges. Our findings suggest that pacemakers exist in the CA3a–b region for the generation of epileptiform discharges in the hippocampus. VPA reduces the conduction of such discharges in the network by reducing the propagation speed.

Keywords: epileptiform discharges; hippocampal slices; microelectrode array; valproate

INTRODUCTION

The epileptic seizure is a dynamic process involving a rapid transition from normal activity to a state of hypersynchronous neuronal discharges. Epileptiform discharges induced in hippocampal slices offer a simple and practical system to study epileptiform pacemaker and propagation mechanisms[1]. The initiation of epileptiform discharges occurs as a progression from local asynchronous to outwardly-spreading synchronous neuronal activity[2]. Intrinsic bursting cells have been shown to play a pivotal role in this process[1,3,4]. Rather than a series of sequential initiations, propagation within local neural networks has been suggested as the basis of transmission of activity through a continuum of neuronal populations[5,6]. The propagation of epileptiform discharges can be understood as a pulse of synchronous activity transmitted from one neuronal population to the next, involving a rapid process during which neighboring neurons are recruited to generate discharges throughout the spatial extent of the network[7]. Previous studies have revealed that an improved understanding of the propagation patterns of epileptiform discharges, such as pathways and speed, could provide valuable insights into understanding the mechanisms of epileptogenesis and lead to better treatment of patients with epilepsy[8-11].

The goal of this study was to characterize the spatiotemporal dynamics of epileptiform propagation and the pharmacological effects of the anti-epileptic drug valproate (VPA) on epileptiform discharges in the hippocampal network. The multi-electrode recording technique, which allows for simultaneous multiple-site recordings, was used to record neuronal activity in hippocampal slices during epileptiform discharges and drug application.

MATERIALS AND METHODS

Chemicals and Drugs

Sodium VPA was from Sigma-Aldrich (St. Louis, MO), and other chemicals were from Sinopharm Chemical Reagent Co., Ltd (Shanghai, China). Chemicals were prepared as stock solutions and stored in tightly-sealed vials at the recommended temperature. During experiments, the drugs were dissolved in high-K^+ artificial cerebrospinal fluid (ACSF).

Hippocampal Slice Preparation

Hippocampal slices were prepared from male Sprague-Dawley rats at postnatal days 14–21, obtained from the Shanghai Institutes for Biological Sciences. All animal experiments were performed in accordance with the regulations of the Ethics Committee (2012027), School of Biomedical Engineering, Shanghai Jiao Tong University. All efforts were made to minimize the suffering of animals. Briefly, after cervical dislocation and decapitation, the brain was quickly removed and placed in 0–4°C ACSF of the following composition (in mmol/L): NaCl 124, KCl 3.5, NaH_2PO_4 1.2, $MgCl_2{\cdot}6H_2O$ 1.3, $CaCl_2$ 2, $NaHCO_3$ 25, and *D*-glucose 10 at pH 7.4 (~300 mOsm/L), gassed with a mixture of 95% O_2 and 5% CO_2. Transverse hippocampal slices (400 μm) were prepared with a vibratome (Series 1000, Sectioning Systems, Vibratome, St. Louis, MO) and incubated in oxygenated (95% O_2 + 5% CO_2) ACSF at room temperature (25–27°C) for at least 2 h before use[12]. Epileptiform discharges were induced by high-K^+ ACSF with the following composition (in mmol/L): NaCl 119, KCl 8.5, NaH_2PO_4 1.2, $MgCl_2{\cdot}6H_2O$ 1.3, $CaCl_2$ 2, $NaHCO_3$ 25, and *D*-glucose 10 at pH 7.4 (~300 mOsm/L), gassed with a mixture of 95% O_2 and 5% CO_2[13].

Experimental Systems

The micro-electrode array (MEA) consisted of 60 electrodes (30 μm in diameter) arranged in an 8 × 8 matrix (leaving the 4 corners void) with 200 μm tip-to-tip distances (horizontal and vertical). The slice was placed in the center of the MEA[13]. A nylon mesh was carefully placed on the slice to immobilize it. The MEA with the slice was quickly transferred to the stage of an Olympus microscope. The slice was perfused continuously with oxygenated ACSF at 0.8 mL/min with a peristaltic pump (Ismatec SA, Glattbrugg, Switzerland) during the whole recording session. The perfusate was pre-warmed to 27°C in a water-bath. The temperature of the MEA chamber was maintained at 35°C with a temperature-control unit (Thermostat HC-X, Multichannel Systems GmbH, Germany).

MEA Recordings

All data were recorded with an MEA with a 60-channel amplifier (single-ended, bandwidth 1 Hz–3.4 kHz, amplification 1200×, input impedance >10^{10} Ω, output impedance 330 Ω), connected to a 60-channel A/D card. An Ag/AgCl wire was immersed in the bath solution and acted as the reference electrode. The relative position of the slice on the MEA was ascertained by observation under a light microscope (Olympus, Japan). The recorded areas and electrical signals from all electrodes are illustrated in Fig. 1. The anatomical criteria for identifying the hippocampal sub-regions were taken from previous studies on the cornu ammonis (CA)[14]. All signals were sampled at 20 kHz and stored on a PC for offline analysis.

Data and Statistical Analysis

Raw data were taken for offline analysis using MC-Rack (Multichannel Systems GmbH, Germany) and MATLAB (MathWorks, USA) softwares. As in previous studies[10,15], the electrical signals detected by each electrode of the MEA were separated into field potentials (FPs) and multi-unit activity (MUA) by 1–100 Hz band-pass (EEG band) and 200 Hz high-pass filtering, respectively. FPs and MUA were determined when the negative phase of the signal exceeded four times the standard deviation from the mean value of a 500-ms baseline. Burst durations and frequencies were obtained by averaging data recorded by two adjacent electrodes located in each sub-region (CA3a, CA3b, CA3c and CA1) along the pyramidal layer. To analyze the initiation and propagation of epileptiform discharges, data from all electrodes along the pyramidal layer were used. The relative onset times of the two components were defined as the time points when the signal overshot the threshold in their respective frequency ranges. As suggested in previous studies[10,15], the initiation and propagation of the FP can be judged by comparing the occurrence time of its primary negative peak recorded along the pyramidal cell layer. To quantify the synchronization of neuronal activity during seizures, cross-correlation analysis of MUA was also applied to determine the relationship between signals

recorded from neighboring regions[10]. Briefly, the spike trains were represented as "0–1" sequences (bin-width = 1 ms), where "1" means that there is one spike in the time bin of interest and "0" means that there is no spike in that bin. Then the normalized cross-correlation function was applied in accordance with previous reports[16] as follows:

$$C_{xy}(m)=\begin{cases}\dfrac{\sum_{n=0}^{N-|m|-1}x_n y_{n+m}}{R} & R=\sqrt{\sum x_i^2\sum y_i^2} \quad m\geq 0\\ C_{yx}(-m) & m<0\end{cases}.$$

Measurements are expressed as mean ± SEM in the text. Statistical comparisons were made using Student's *t*-test or one-way ANOVA with a significance level of $P<0.05$ (SPSS 13.0).

RESULTS

Properties of High-K^+-Induced Epileptiform Discharges

After the hippocampal slices were exposed to high-K^+ (8.5 mmol/L) ACSF for 10–15 min, repetitive epileptiform discharges were recorded from all CA regions (Fig. 1B). The repetitive discharges appeared at intervals of 2–15 s and consisted of an FP and a cluster of MUA which were superimposed on the FP (Fig. 1C).

The neuronal firing activity recorded from different sub-regions became synchronized after the high-K^+-induced epileptiform discharges began. Two parameters were used to quantify the bursting activity (MUA): burst count per minute and burst duration. After stable discharges were induced by increased $[K^+]_o$ (at least 10 min after the appearance of

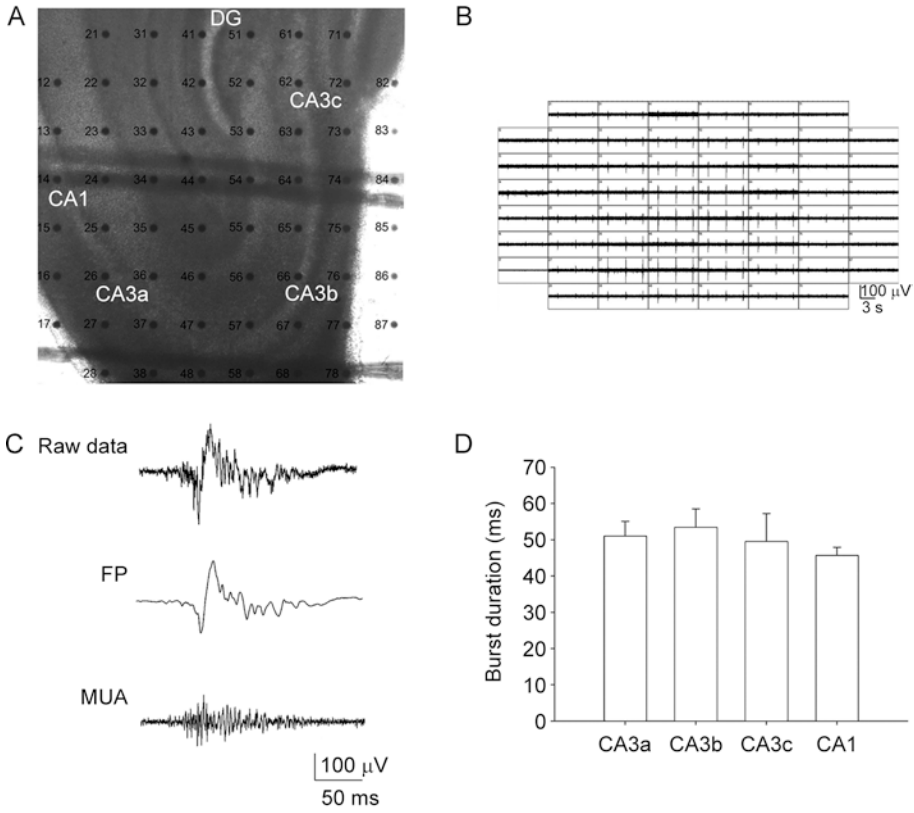

Fig. 1. Epileptiform discharges induced by high-K^+ artificial cerebrospinal fluid. A: An acute hippocampal slice mounted on an MEA. Each black dot represents one electrode. The slice is divided into CA3c, CA3b, CA3a, CA1 and DG sub-regions. B: Typical MEA recording of epileptiform discharges from the slice shown in (A). Each data window shows the recording from one electrode. C: Example of a single epileptiform discharge evoked by 8.5 mmol/L $[K^+]_o$ recorded by electrode 37 (E37) with signals recorded at the CA3 pyramidal cell layer before (top trace), and after filtering for field potential (FP) components (1–100 Hz band-pass filter, middle trace) and multi-unit activity (MUA; 200 Hz high-pass filter, bottom trace). D: Duration of high-K^+-induced MUA from pyramidal cells of different CA regions. Mean values of durations were calculated based on 10-min recording of stable discharges (n = 5 slices). There were no significant differences among the MUA durations in different sub-regions (ANOVA).

discharges), burst activity occurred through the whole slice synchronously with burst durations ranging from 30 to 100 ms. Burst frequency was 20.2 ± 2.8 bursts/min (n = 5 slices). The durations of the bursts from different CA regions were: 51.0 ± 4.1 ms for CA3a, 53.4 ± 5.1 for CA3b, 49.5 ± 7.8 for CA3c, and 45.6 ± 2.3 for CA1 (P >0.05, ANOVA for repeated measures, n = 5 slices; Fig. 1D). Perfusion of these slices with normal ACSF (~5 min) quickly abolished most of the spontaneous activity (n = 5 slices).

Initiation and Propagation of High-K^+-Induced Epileptiform Discharges in Hippocampal Slices

We next investigated the initiation and propagation of the epileptiform discharges. Fig. 2 shows an example from a representative slice. Electrodes E68, E67, E75, E74, E63, E43, E34, E25 and E16 situated at the pyramidal cell layer were chosen for analyzing the initiation and propagation of the discharges (Fig. 2A). By comparing the timing of the negative peaks of the FPs, we found that the initiation site of the discharges along the pyramidal cell layer in this slice was in the CA3a area, and the discharges spread bi-directionally to the CA1 and CA3c regions (Fig. 2B). The MUA recorded from different sub-regions became synchronized after the high-K^+-induced discharges appeared. Cross-correlation analysis was used to compare the relative time delays of the synchronized MUA (Fig. 2C shows representative cross-correlation histograms derived from electrodes E68, E74, E43 and E16 located in the CA3a, CA3b, CA3c and CA1 sub-regions along the pyramidal layer). Positive time-delays indicated that CA3a (E74) signals preceded firing in other CA sub-regions, indicating that the initiation site of epileptiform discharge was in CA3a in this slice.

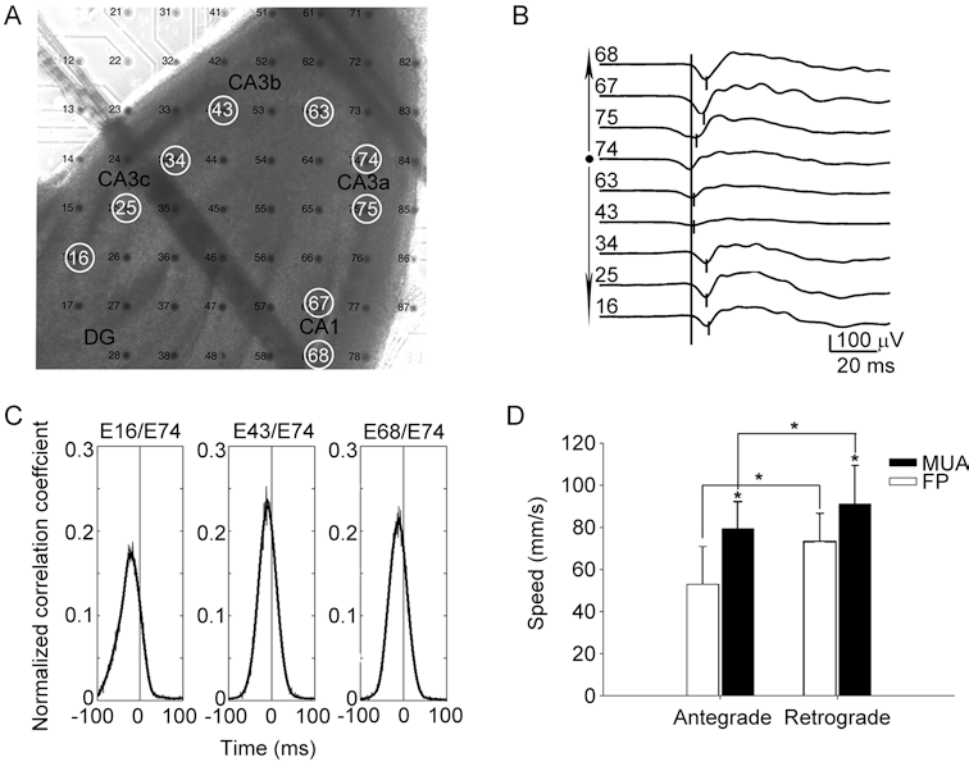

Fig. 2. Initiation and propagation of epileptiform discharges induced by high-K^+ artificial cerebrospinal fluid. A: Representative hippocampal slice and positions of the electrodes. Electrodes E68, E67, E75, E74, E63, E43, E34, E25 and E16 situated along the pyramidal cell layer were chosen for analyzing the initiation and propagation of the discharges. B: Relative timing of the negative peaks of field potentials (FPs) showed that the discharges initiated from CA3a (E74) and propagated to CA3c and CA1. C: Cross-correlation of multi-unit activity (MUA) in CA3a *versus* other CA areas showed the relative time delays of the signals after 8.5 mmol/L $[K^+]_o$ application (binwidth = 1 ms). D: Statistics of propagation speeds measured from FPs and MUA showed that anterograde propagation speeds were slower than retrograde speeds (n = 5, *P <0.05, paired t-test).

This is compatible with the direct comparison of negative peaks of the FPs presented in Fig. 2B. Data from five slices showed that the discharges presented similar bi-directional propagation patterns. The discharges were initiated in the CA3a–b sub-regions and propagated to the CA1 and CA3c sub-regions. The time-delays of FPs and MUA between electrodes were measured to calculate the propagation speeds of the discharges. We found that the time delays of these two components both increased in proportion to the distance (defined as the length of pyramidal cell layer between recording electrodes, Fig. 2D). In the example shown in Fig. 2A, the anterograde (CA3a–b to CA1) speeds were 63.2 mm/s (FP) and 66.8 mm/s (MUA), and the retrograde (CA3a–b to CA3c) speeds were 69.0 mm/s (FP) and 92.2 mm/s (MUA). Comparing the propagation speeds of the FP and MUA, we found that highly synchronous MUA propagated faster than FPs from the initiation site to the other sites [anterograde: 53.0 ± 18.0 mm/s (FP), 70.8 ± 22.4 mm/s (MUA), t =–6.182, df =97, P =0.0000; retrograde: 73.5 ± 13.1 mm/s (FP), 99.7 ± 26.2 mm/s (MUA), t = –8.993, df = 97, P = 0.0000, paired t-test, n = 5 slices; Fig. 2D]. In addition, both MUA and FPs showed faster retrograde than anterograde propagation (FP, t = –8.812, df = 97, P = 0.0000; MUA, t = –8.626, df = 97, P = 0.0000, paired t-test).

To confirm the existence of pacemakers in the CA3 sub-area, we performed another set of experiments on slices in which the Schaffer collaterals between CA3 and CA1 were cut. The results showed that this abolished FPs as well as MUA in CA1, while neither the initiation nor the propagation direction of the discharges within the CA3 sub-region was affected (Fig. 3). Similar results were obtained from another two slices.

Pharmacological Effects of VPA on High-K^+-Induced Epileptiform Discharges

After the establishment of stable epileptiform discharges for at least 10 min, sodium VPA (100 μmol/L) was applied[17] to the slice. Burst frequency, burst duration and propagation speeds in the slice were measured before, during and after VPA application. In one typical slice, the frequencies of epileptiform discharges before, during and after VPA application were 14/min (control), 20/min (VPA) and 22/min (washout) respectively. The durations of the discharges were 63.4 ms (control), 61.6 ms (VPA) and 61.9 ms (washout). The statistical results showed that neither the burst frequency nor the duration of discharges was influenced by

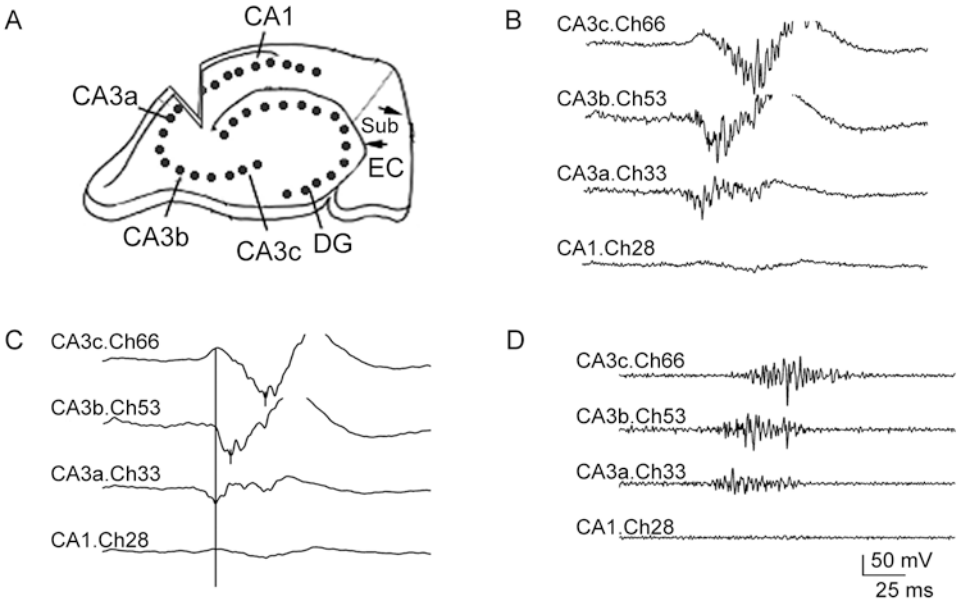

Fig. 3. Sectioning the Schaffer collaterals between CA3 and CA1 abolished epileptiform discharges in CA1 but not in CA3. A: Schematic diagram of experimental incision. B–D: Raw data (B), FPs (C) and MUA (D) of discharges recorded by electrodes in the CA3c, CA3b, CA3a and CA1 sub-regions after sectioning Schaffer collaterals between CA3 and CA1. Some of the positive wave was erased in order to highlight the negative wave.

the application of VPA for 15–20 min (Fig. 4).

The effects of VPA on the bi-directional propagation speeds were measured by comparisons of FP negative peaks and cross-correlation analysis of time delays measured from MUA. The anterograde and retrograde speeds during and after 100 μmol/L VPA application in a typical slice are presented in Table 1. The anterograde speed was not significantly influenced by the application of VPA, but the retrograde speed decreased during VPA perfusion. The VPA-induced suppression of retrograde propagation speed of epileptiform discharges partially recovered after 15–30 min of drug washout (P <0.05, paired t-test, n = 5 slices; Fig. 4, Table 2).

Table 1. The bi-directional propagation speeds (mm/s) of a typical slice

	FP		MUA	
	Anterograde	Retrograde	Anterograde	Retrograde
High-K^+	65.0	40.1	44.5	76.2
VPA	48.2	29.8	40.2	12.9
Washout	50.6	40.3	41.7	51.5

FP, field potential; MUA, multi-unit activity; VPA, valproate.

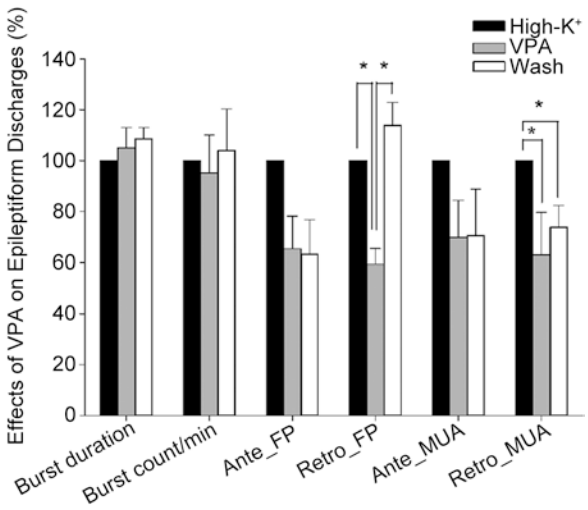

Fig. 4. Effects of 100 μmol/L sodium valproate (VPA) on high-K^+-induced epileptiform discharges. Burst duration, burst frequency and propagation speeds before, during and after application of 100 μmol/L VPA. All data were normalized to the parameters during stable discharges before drug application. Ante: anterograde propagation speed; FP, field potential; MUA, multi-unit activity; Retro: retrograde propagation speed. *P <0.05, paired t-test, n = 5 slices.

DISCUSSION

Application of MEA to Recording Epileptiform Discharges *in vitro*

The application of MEA has greatly facilitated studies of the spatiotemporal properties of local networks in epileptiform discharges[12,16,18-20]. Similar to the signals recorded with traditional electrodes[10,15], epileptiform discharges are recorded as MUA characterized by a rapid series of action potentials superimposed on an FP (Fig. 1C). These discharges are thought to have a common electrophysiological basis with the interictal spikes on the EEG *in vivo*[10]. MEA offers the possibility of monitoring the epileptiform discharges in different sub-regions of rat hippocampal slices and thus provides information on the spatiotemporal dynamics of these discharges.

In order to investigate the spatiotemporal characteris-

Table 2. Statistical results of VPA effects on high-K^+-induced epileptiform discharges

	Burst frequency (%)	Burst duration (%)	Propagation speed (%)			
			FP		MUA	
			Anterograde	Retrograde	Anterograde	Retrograde
High-K^+	100	100	100	100	100	100
VPA	95.2 ± 14.9	105.1 ± 7.9	65.4 ± 12.8	59.4 ± 6.1	69.8 ± 14.6	63.0 ± 16.6
Washout	104.0 ± 16.3	108.7 ± 4.3	63.3 ± 13.5	113.9 ± 9.0	70.6 ± 18.2	73.9 ± 8.5

FP, field potential; MUA, multi-unit activity; VPA, valproate.

tics and dynamics of the induced epileptiform discharges, the hippocampal slices were divided into CA3c, CA3b, CA3a, CA1 and DG sub-regions according to the cytoarchitecture reported in previous studies[1]. In the present study, the burst durations and frequencies were averaged from data recorded by two adjacent electrodes located in each sub-region (CA3a, CA3b, CA3c and CA1) along the pyramidal cell layer. Data from all electrodes along the pyramidal layer were used for analyzing the initiation and propagation of the discharges. The main results of our study were that: (1) discharges were predominantly initiated in the CA3a–b region, and propagated bi-directionally to the CA1 and CA3c areas when the slices were exposed to high-K^+; (2) disconnection of CA3 from CA1 abolished the discharges in CA1 without disrupting the initiation of discharges in CA3; and (3) when 100 μmol/L sodium VPA was added, the speed of the high-K^+-induced propagation was reduced, but the rate and duration of discharges were not influenced.

Firing Patterns of Epileptiform Discharges

A recurrent network of excitatory connections, excited by the activation of non-NMDA and NMDA glutamatergic ionotropic receptors, rapidly recruits neurons into the burst onset[4]. Burst activity in the hippocampus can also induce long-term changes in functional synaptic connections, including the potentiation of excitatory synapses between pyramidal neurons and potential functional decreases in inhibitory synaptic connections[21,22]. The comprehensive effect of these changes is to enhance the excitability of the neuronal network, and they play significant roles in epileptogenesis. Neuronal burst activity occurs in various epilepsy models[3,15,23]. In our study, large-scale synchronous epileptiform discharges composed of MUA and FPs emerged abruptly after perfusion with high-K^+ ACSF (Fig. 1C), with MUA reflecting the excitability in a small group of neurons and FPs in the EEG band representing synaptic interaction[24]. Cross-correlation analyses based on MUA recorded from different electrodes showed time delays of the activity in different areas, which indicated the propagation of neuronal discharges from the initiation site to the surrounding areas. On the other hand, repetitive synchronized discharges were observed at intervals of 2–15 s in slices during continuous superfusion with high-K^+ ACSF. A previous study had suggested that the interval between epileptiform discharges depends on the time-course of vesicle replenishment after a burst[25]. Therefore, cell firings (MUA) and synaptic activity (FPs) were both involved in the generation of the discharges.

Initiation of Epileptiform Discharges in Acute Hippocampal Slices

Many regions have been identified as initiation sites of epileptiform discharges *in vitro*, including CA3[1,10,26], entorhinal cortex[27] and subiculum[28]. Different experimental methods, epileptic models or animal strains could account for the identification of different epileptogenic foci[29,30]. In the present study, we specifically focused on high-K^+ ACSF-induced epileptiform discharges in hippocampal slices using MEA recordings. The initiation site of the discharges was determined by comparing the time-delays of negative peaks of FPs as well as cross-correlations of MUA timing. Our results showed that the initiation site along the pyramidal cell layer was in the CA3a–b sub-region (Fig. 2). Sectioning the Schaffer collaterals between CA3 and CA1 abolished the bursting activity in CA1, but had no effect on the firing activity in CA3 (Fig. 3). These results indicate that the discharges induced by 8.5 mmol/L $[K^+]_o$ arise from the CA3a–b sub-area in the slice, compatible with previous reports that pacemaker neurons in these sub-areas play a critical role in the initiation of hippocampal epileptiform discharges[1,10].

Propagation Patterns of Epileptiform Discharges in Acute Hippocampal Slices

Two propagation patterns of epileptiform discharges have been reported in hippocampal slices: unidirectional or bi-directional propagation initiated from the CA3 region[10,27]. Our results showed that epileptiform discharges induced by high-K^+ in rat hippocampal slices propagated bi-directionally from the initiation site (CA3a–b) to the CA1 and CA3c sub-areas. In the propagation process, a small excitatory synaptic input to the follower site can recruit a subset of the neuronal population, mostly bursters, into firing. Once a critical number of neurons are recruited into the discharge zone, the activity of their neighboring neurons becomes synchronous and spatially integrated. The propagation speed of epileptiform discharges is dependent on the integration time required to bring the successive neurons to firing threshold, which is influenced by the structure of the network, synaptic efficiency and the biophysical properties of the cell membrane[4]. The more quickly each neighboring

neuron is recruited, the faster the discharge may propagate[8].

NMDA and non-NMDA receptors (AMPA receptors and kainate receptors) are the main glutamatergic receptors involved in epilepsy. Studies have reported that NMDA-receptor-dependent discharges propagate at about one fifth of the conduction velocity of non-NMDA-receptor-dependent events[9]. We found that MUA and FPs recorded from different electrodes along the pyramidal cell layer both showed high temporal correlation during epileptiform discharges (Fig. 2B, C). FPs propagated slower than MUA (Fig. 2D), which suggests the presence of FP/spike dissociation during epileptiform synchronization; this has been found during the induction of long-term potentiation in the hippocampus[31]. In our study, the discharges were initiated in the CA3a–b region, and propagated to CA1 (anterograde) and CA3c (retrograde). When non-NMDA and NMDA receptors were activated in the high-K^+ model, interictal activity showed faster retrograde than anterograde propagation (Fig. 2D). A previous study showed different regional expression of AMPA receptor subunits along the two pathways of the hippocampal pyramidal layer[32]. Therefore, we postulate that the anterograde propagation (from CA3a–b to CA1) might be preferentially mediated by NMDA-receptor-dependent transmission, while non-NMDA-receptor-mediated transmission plays a more important role in the retrograde propagation (from CA3b to CA3c) in the hippocampal loop.

Effects of VPA on High-K^+ACSF-Induced Epileptiform Discharges

VPA is one of the major antiepileptic drugs commonly used in clinical practice. During bath application of VPA at a level comparable to the concentration in cerebrospinal fluid for chronic treatment in human brain[17], some aspects of the epileptiform discharges (e.g. burst frequency and duration) were not influenced (Fig. 4). Similar results have been found in the 4-aminopyridine model[33,34]. These findings are in line with clinical evidence obtained by investigating the relationship between the interictal spiking rate and antiepileptic drug levels, which found that drug levels that influence seizure occurrence do not decrease the spiking rate (interictal epileptiform discharges)[35]. In the present study, we also found that VPA at a clinically-relevant concentration was sufficient to suppress the retrograde propagation of epileptiform discharges, but did not significantly affect the anterograde propagation speed (Fig. 4). Dzhala *et al.* reported that the transition from interictal activity to ictal-like sustained epileptiform discharges is preceded by an increase in the speed of discharge propagation[10]. So our results imply that VPA at 100 μmol/L can prevent the occurrence of ictal discharges by reducing the retrograde propagation speed of interictal epileptiform discharges.

In our experiments, we found that the bi-directional propagation speeds of epileptiform discharges in hippocampal slices were different (Fig. 2D). In the VPA application experiments, the effects of VPA on propagation speeds also showed differences in the two directional pathways (Fig. 4). As VPA suppresses the responses mediated by glutamate receptors (NMDA receptors)[36], the more glutamate receptors present, the stronger the effects of VPA. So we postulate that the effects of VPA on bi-directional propagation speed may reflect its inhibitory effects on the glutamate receptors. This implies that VPA should be used even in the chronic period, especially when interictal spiking is still observed in the EEG.

ACKNOWLEDGEMENTS

This work was supported by the Natural Science Foundation of Shanghai (11ZR1421800, 12ZR1413800) and the Shanghai Jiao Tong University Fund for Interdisciplinary Research for Medical Applications (G08PETZD05).

Received date: 2012-06-05; Accepted date: 2012-08-20

REFERENCES

[1] Wittner L, Miles R. Factors defining a pacemaker region for synchrony in the hippocampus. J Physiol 2007, 584: 867–883.

[2] Miles R, Wong RK. Single neurones can initiate synchronized population discharge in the hippocampus. Nature 1983, 306: 371–373.

[3] Jensen MS, Yaari Y. Role of intrinsic burst firing, potassium accumulation, and electrical coupling in the elevated potassium model of hippocampal epilepsy. J Neurophysiol 1997, 77: 1224–1233.

[4] McCormick DA, Contreras D. On the cellular and network bases of epileptic seizures. Annu Rev Physiol 2001, 63: 815–846.

[5] Ermentrout B. The analysis of synaptically generated traveling waves. J Comput Neurosci 1998, 5: 191–208.

[6] Wu JY, Guan L, Tsau Y. Propagating activation during oscillations and evoked responses in neocortical slices. J Neurosci

1999, 19: 5005–5015.

[7] Golomb D, Amitai Y. Propagating neuronal discharges in neocortical slices: computational and experimental study. J Neurophysiol 1997, 78: 1199–1211.

[8] Trevelyan AJ, Sussillo D, Yuste R. Feedforward inhibition contributes to the control of epileptiform propagation speed. J Neurosci 2007, 27: 3383–3387.

[9] Telfeian AE, Connors BW. Epileptiform propagation patterns mediated by NMDA and non-NMDA receptors in rat neocortex. Epilepsia 1999, 40: 1499–1506.

[10] Dzhala VI, Staley KJ. Transition from interictal to ictal activity in limbic networks *in vitro*. J Neurosci 2003, 23: 7873–7880.

[11] Goda M, Kovac S, Speckmann EJ, Gorji A. Glutamate and dopamine receptors contribute to the lateral spread of epileptiform discharges in rat neocortical slices. Epilepsia 2008, 49: 237–247.

[12] Hill AJ, Jones NA, Williams CM, Stephens GJ, Whalley BJ. Development of multi-electrode array screening for anticonvulsants in acute rat brain slices. J Neurosci Methods 2010, 185: 246–256.

[13] Liu JS, Gong XW, Gong HQ, Zhang PM, Liang PJ, Lu QC. Exploring spatiotemporal patterns of epileptiform discharge in hippocampal slice using multi-electrode arrays. Acta physiol Sin 2010, 62: 163–170.

[14] Paxinos G. The Rat Nervous System. San Diego: Elsevier Academic Press, 2004.

[15] de la Prida LM, Huberfeld G, Cohen I, Miles R. Threshold behavior in the initiation of hippocampal population bursts. Neuron 2006, 49: 131–142.

[16] Gong XW, Yang F, Liu JS, Lu QC, Gong HQ, Liang PJ, *et al.* Investigation of the initiation site and propagation of epileptiform discharges in hippocampal slices using microelectrode array. Prog Biochem Biophys 2010, 37: 1240–1247.

[17] Johannessen CU, Johannessen SI. Valproate: past, present, and future. CNS Drug Rev 2003, 9: 199–216.

[18] Novak JL, Wheeler BC. Two-dimensional current source density analysis of propagation delays for components of epileptiform bursts in rat hippocampal slices. Brain Res 1989, 497: 223–230.

[19] Wheeler BC, Novak JL. Current source density estimation using microelectrode array data from the hippocampal slice preparation. IEEE Trans Biomed Eng 1986, 33: 1204–1212.

[20] Yang F, Gong X, Gong H, Zhang P, Liang P, Lu Q. Microelectrode array recordings of excitability of low Mg2+-induced acute hippocampal slices. Neural Regen Res 2010, 5: 1548–1551.

[21] Isaeva E, Isaev D, Khazipov R, Holmes GL. Selective impairment of GABAergic synaptic transmission in the flurothyl model of neonatal seizures. Eur J Neurosci. 2006, 23: 1559–1566.

[22] Debanne D, Thompson SM, Gahwiler BH. A brief period of epileptiform activity strengthens excitatory synapses in the rat hippocampus *in vitro*. Epilepsia 2006, 47: 247–256.

[23] Avoli M, D'Antuono M, Louvel J, Kohling R, Biagini G, Pumain R*, et al.* Network and pharmacological mechanisms leading to epileptiform synchronization in the limbic system *in vitro*. Prog Neurobiol 2002, 68: 167–207.

[24] Cohen I, Miles R. Contributions of intrinsic and synaptic activities to the generation of neuronal discharges in *in vitro* hippocampus. J Physiol 2000, 524 Pt 2: 485–502.

[25] Bains JS, Longacher JM, Staley KJ. Reciprocal interactions between CA3 network activity and strength of recurrent collateral synapses. Nat Neurosci 1999, 2: 720–726.

[26] Colom LV, Saggau P. Spontaneous interictal-like activity originates in multiple areas of the CA2-CA3 region of hippocampal slices. J Neurophysiol 1994, 71: 1574–1585.

[27] Barbarosie M, Avoli M. CA3-driven hippocampal-entorhinal loop controls rather than sustains *in vitro* limbic seizures. J Neurosci 1997, 17: 9308–9314.

[28] Cohen I, Navarro V, Clemenceau S, Baulac M, Miles R. On the origin of interictal activity in human temporal lobe epilepsy *in vitro*. Science 2002, 298: 1418–1421.

[29] Derchansky M, Rokni D, Rick JT, Wennberg R, Bardakjian BL, Zhang L*, et al.* Bidirectional multisite seizure propagation in the intact isolated hippocampus: the multifocality of the seizure "focus". Neurobiol Dis 2006, 23: 312–328.

[30] Weissinger F, Buchheim K, Siegmund H, Heinemann U, Meierkord H. Optical imaging reveals characteristic seizure onsets, spread patterns, and propagation velocities in hippocampal-entorhinal cortex slices of juvenile rats. Neurobiol Dis 2000, 7: 286–298.

[31] Taube JS, Schwartzkroin PA. Mechanisms of long-term potentiation: EPSP/spike dissociation, intradendritic recordings, and glutamate sensitivity. J Neurosci 1988, 8: 1632–1644.

[32] Baude A, Nusser Z, Molnar E, McIlhinney RA, Somogyi P. High-resolution immunogold localization of AMPA type glutamate receptor subunits at synaptic and non-synaptic sites in rat hippocampus. Neuroscience 1995, 69: 1031–1055.

[33] Bruckner C, Stenkamp K, Meierkord H, Heinemann U. Epileptiform discharges induced by combined application of bicuculline and 4-aminopyridine are resistant to standard anticonvulsants in slices of rats. Neurosci Lett 1999, 268: 163–165.

[34] D'Antuono M, Kohling R, Ricalzone S, Gotman J, Biagini G, Avoli M. Antiepileptic drugs abolish ictal but not interictal epileptiform discharges *in vitro*. Epilepsia 2010, 51: 423–431.

[35] Spencer SS, Goncharova, II, Duckrow RB, Novotny EJ, Zaveri HP. Interictal spikes on intracranial recording: behavior, physiology, and implications. Epilepsia 2008, 49: 1881–1892.

[36] Gean PW, Huang CC, Hung CR, Tsai JJ. Valproic acid suppresses the synaptic response mediated by the NMDA receptors in rat amygdalar slices. Brain Res Bull 1994, 33: 333–336.